



## Molecular Crystals and Liquid Crystals Science and Technology. Section A. Molecular Crystals and Liquid Crystals

Publication details, including instructions for authors and  
subscription information:

<http://www.tandfonline.com/loi/gmcl19>

## Nonlinear Waves Induced by Molecular Flow in Liquid Crystals

Chia-Rong Sheu<sup>a</sup> & Ru-Pin Pan<sup>a</sup>

<sup>a</sup> Department of Electrophysics, National Chiao Tung University,  
Hsinchu, 300, Taiwan, Republic of China

Version of record first published: 04 Oct 2006.

To cite this article: Chia-Rong Sheu & Ru-Pin Pan (1995): Nonlinear Waves Induced by Molecular Flow in Liquid Crystals, Molecular Crystals and Liquid Crystals Science and Technology. Section A. Molecular Crystals and Liquid Crystals, 265:1, 257-269

To link to this article: <http://dx.doi.org/10.1080/10587259508041697>

PLEASE SCROLL DOWN FOR ARTICLE

Full terms and conditions of use: <http://www.tandfonline.com/page/terms-and-conditions>

This article may be used for research, teaching, and private study purposes. Any substantial or systematic reproduction, redistribution, reselling, loan, sub-licensing, systematic supply, or distribution in any form to anyone is expressly forbidden.

The publisher does not give any warranty express or implied or make any representation that the contents will be complete or accurate or up to date. The accuracy of any instructions, formulae, and drug doses should be independently verified with primary sources. The publisher shall not be liable for any loss, actions, claims, proceedings, demand, or costs or damages whatsoever or howsoever caused arising directly or indirectly in connection with or arising out of the use of this material.

## NONLINEAR WAVES INDUCED BY MOLECULAR FLOW IN LIQUID CRYSTALS

CHIA-RONG SHEU and RU-PIN PAN

Department of Electrophysics, National Chiao Tung University, Hsinchu,  
Taiwan 300, Republic of China

**Abstract** Two kinds of thermotropic liquid crystals (5CB and MBBA) are used to study the director nonlinear waves induced by flow in a homeotropic nematic cell. The flow is induced by an exciter, a piece of moving mylar film at one end of the cell. Wave velocities for various exciter velocities and temperatures are measured. A "phase" diagram with our experimental results is constructed and compared with theoretical prediction of reentrant solitons. Waves generated in a first nematic region are observed to be able to penetrate an isotropic region and reappear in a second nematic region.

### 1. INTRODUCTION

It is interesting to study the wave phenomena in nonlinear dynamical systems, such as nematic liquid crystals. Hydrodynamic properties of nematics are described successfully by Ericksen-Leslie continuum theory.<sup>1,2</sup> Under suitable conditions, solitary waves can exist in nematics. There have been extensive studies in both theory and experiments.<sup>3-6</sup> Experimentally, these solitary waves can be generated by using either electric or magnetic field<sup>7</sup> or by molecular flow,<sup>8,9</sup> and can be observed optically.

In 1982, Lam et al. first predicted the existence of propagating solitons in the homeotropic nematic cell under uniform shear flow.<sup>3,9,10</sup> They predicted the existence of several types of solitary waves. Type A soliton, in particular, contains vertical molecules and can be observed as dark line under white light and crossed polarizers. An experiment was carried out by Zhu in the homeotropic cell with a mylar film moving at one end of the cell.<sup>8</sup> Three propagating dark lines were observed. Recently, Lam predicted that there will be a phenomenon of reentrant solitons in the homeotropic cell, if the boundary effect of the cell plates is taken into account.<sup>11</sup> He made some simplifications about the wave equation and reduced it to an effective equation of one spatial dimension with only two dimensionless parameters  $\beta$  and  $\gamma$ . When  $\beta$  is fixed

within a certain narrow range, a sequence of soliton-no soliton-soliton is obtained as  $\gamma$  is varied continuously.

In this study we use the same experimental setup as that in Ref. 8. Two kinds of thermotropic nematics, 5CB (4-n-pentyl-4'-cyanobiphenyl) and MBBA (N-(p-methoxybenzylidene)-p-n-butylaniline), are used in our experiments, and some differences in nonlinear wave properties are found between 5CB and MBBA. Our experimental results are discussed in relation to the prediction of reentrant solitons by Lam. Observation of the wave penetrating through an isotropic liquid region is presented.

## II. EXPERIMENTS

In our experiments, the cell is made with two pieces of floating glass (size: 30 cm length, 5 cm width, 0.5 cm thickness). The cell configuration is shown in Figure 1. There are mylar films put between glasses for three purposes. The spacer mylar films fix the nematic layer thickness. The exciter mylar film induces the Poiseuille flow in the cell. The side mylar films reduce the flow in the z-direction. The glasses are coated with DMOAP (n-octadecyldimethyl [3-(trimeth-oxy-silyl)-propyl] ammonium chloride) to make the homeotropic alignment for the nematics.<sup>12</sup> The volume concentrations of DMOAP are 0.01% and 1% for the MBBA cell and the 5CB cell, respectively.

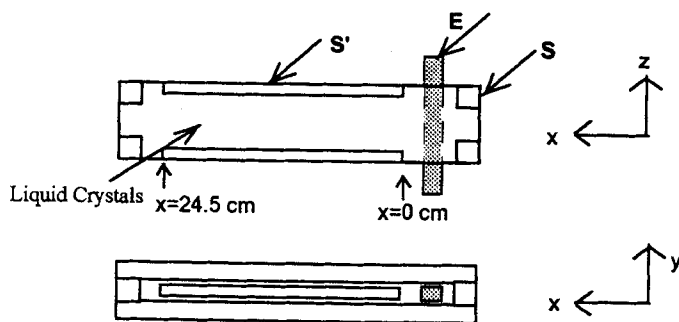


FIGURE 1 Liquid crystal cell. E is the exciter mylar film, S is the spacer mylar film and S' is for side mylar film.

The experimental setup is shown in Figure 2. A fluorescent lamp illuminates the cell. A polarizer is placed below the cell with polarization direction at an angle  $45^\circ$  to the x-direction, and a crossed analyzer is placed above the cell. Finally, a video camera is used to record the experimental process in VCR tapes. We use a motor to push (move to the positive x-direction) or to pull (move to the negative x-direction) the exciter, which moves uniformly in an 1 cm region and induces the Poiseuille flow. The moving

exciter is the dynamical source of the waves. By changing the cell temperature or the exciter velocity, we observe various nonlinear waves. We use two kinds of thermotropic nematics: 5CB and MBBA. The cell temperature is maintained with two heating rods placed in the box, in which the cell is placed. The uniformity of the cell temperature is within  $\pm 1^\circ\text{C}$  for the whole cell; the central part of the cell is always slightly higher in temperature. We analyze the VCR tapes to obtain the wave velocities. We have also carried out the experiments when the middle of the cell is in the isotropic liquid phase while the two end regions are still in nematic phase.

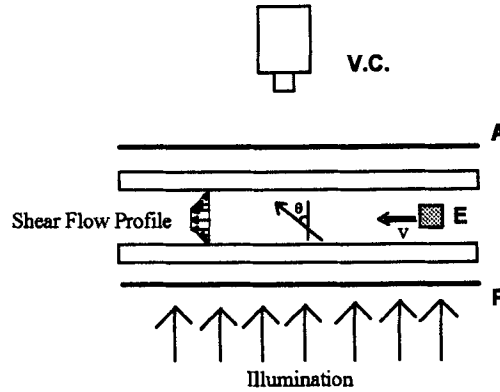


FIGURE 2 Experimental Setup. P is for polarizer, E is for moving exciter mylar film, A is for analyzer, and V.C. is for video camera.

### III. THEORY

With Ericksen-Leslie continuum theory and some assumptions (including  $\theta = \theta(x, t)$  which is the angle between the nematic director and the  $y$ -axis, homeotropic nematic cell,  $S = \partial\psi/\partial y = \text{constant}$ , one-elastic-constant approximation,  $\mathbf{n} = (\sin\theta, \cos\theta, 0)$ ,  $\mathbf{v} = (v(y), 0, 0)$ , and  $d\theta/dt \approx \partial\theta/\partial t$ ), Lam et al. got an equation describing the director motion in simple shear, the nonlinear driven damped sine-Gordon equation, and predicted the existence of solitary waves under suitable conditions.<sup>3,10</sup> The wave equation is found to be

$$M \frac{d^2\theta}{dt^2} = K \frac{\partial^2\theta}{\partial x^2} - \gamma_1 \frac{d\theta}{dt} + \frac{S}{2} (\gamma_1 - \gamma_2 \cos 2\theta), \quad (1)$$

where  $M$  is the molecular moment of inertia,  $K$  is the elastic constant,  $S = \partial\psi/\partial y = \text{constant}$ ,  $\gamma_1$  and  $\gamma_2$  are the viscosity coefficients. The above equation possesses several solitary wave solutions.<sup>10</sup>

Recently, Lam considered a two dimensional analysis with the effect of boundaries of the cell plates included. The equation becomes<sup>11</sup>

$$M \frac{d^2\theta}{dt^2} = K \left( \frac{\partial^2\theta}{\partial x^2} + \frac{\partial^2\theta}{\partial y^2} \right) - \gamma_1 \frac{d\theta}{dt} + \frac{S}{2} (\gamma_1 - \gamma_2 \cos 2\theta) . \quad (2)$$

For the Poiseuille flow,  $\theta(x,y,t)=f(y)\theta_m(x,t)$ ,  $f(y)=g(y)/g(-y_m)$ , where  $g(y)=2y/d-\sin(\pi y/d)$ ,  $y_m=(d/\pi)\cos^{-1}(2/\pi)\approx 0.28d$  ( $d$  is the thickness of nematic layer),  $\theta_m$  is the maximum  $\theta$  across the  $y$ -direction at  $-y_m$ . An effective equation of motion, with  $M$  ignored, is given in the dimensionless form as follows.

$$\frac{\partial\theta_m}{\partial T} = \frac{\partial^2\theta_m}{\partial X^2} - 2\beta\theta_m + \gamma + \cos 2\theta_m , \quad (3)$$

where  $T=t/\tau$ ,  $\tau=2\gamma/S_m$ ,  $X=x/\lambda$ ,  $\lambda=[2K/(|\gamma_2|S_m)]^{1/2}$ ,  $\gamma=\gamma_1/|\gamma_2|$ ,  $\beta=KB\pi^2/(S_md^2|\gamma_2|)$ ,  $S_m=S(-y_m)\sim\mathcal{U}/(d/3)$ ,  $B=-(d/\pi)^2 f''(-y_m)\approx 3.66$ . Here  $\mathcal{U}$  is the maximum velocity in a Poiseuille flow. The steady uniform states of Eq.(3), with only two dimensionless parameters  $\beta$  and  $\gamma$  in the equation, are given by

$$\cos(2\theta_m) - (-\gamma + 2\beta\theta_m) = 0 . \quad (4)$$

Lam made numerical analyses about soliton solutions and got the  $\beta$ - $\gamma$  phase diagram (Figure 3 in reference 11) to show the region where solitons existed. This phase diagram will be drawn with our experimental data in the Sec. V. When  $\beta$  is fixed within a certain narrow region, one can observe the sequence soliton-no soliton-soliton as  $\gamma$  is varied, i.e., a reentrant soliton phenomenon. For example, in the Poiseuille flow, when the elastic constant  $K\sim 10^{-6}$  dyn,  $|\gamma_2|\sim 1$  P, and  $\mathcal{U}\sim 1$  mm/sec, the reentrant region occurs when the thickness of nematic layer is between 32  $\mu\text{m}$  and 50  $\mu\text{m}$ .

#### IV. EXPERIMENTAL RESULTS

##### Waves in MBBA cell

The cell is made with 50  $\mu\text{m}$  spacer mylar films, 35.5  $\mu\text{m}$  side mylar films, and 23  $\mu\text{m}$  exciter mylar film. The temperature of the cell  $T$  is fixed between 21°C and 33°C, and the exciter velocity  $V=V\hat{e}_x$  is fixed with  $|V|$  between 0.4 mm/sec and 1.0 mm/sec.  $V>0$  ( $<0$ ) corresponds to the exciter moving toward the left (right) in all figures.

Within the  $V$  and  $T$  ranges above, three dark lines can be observed clearly during the period when the exciter is moving. These lines are created one by one near the exciter, and move toward the other end of the cell (see Figure 3). The width of the early appearing dark line is wider and darker than the later appearing one. For example, the widths of the three dark lines are 4mm, 3mm, 2mm, respectively, when  $T=25^\circ\text{C}$  and  $V=1$  mm/sec. When  $V$  is reduced below 0.4 mm/sec the dark lines are unstable, distorted very badly, and disappear during the experimental process.



**FIGURE 3** The picture for MBBA cell at 30°C with  $V = -1.0$  mm/sec . Three dark lines can be observed clearly near the left end (the end away from the exciter mylar film). See Color Plate IX.

We find that the shapes of the dark lines are more stable when  $V < 0$  (Figure 4) than those when  $V > 0$  (Figure 5). With higher  $V$ , the lines can travel farther away from the exciter.

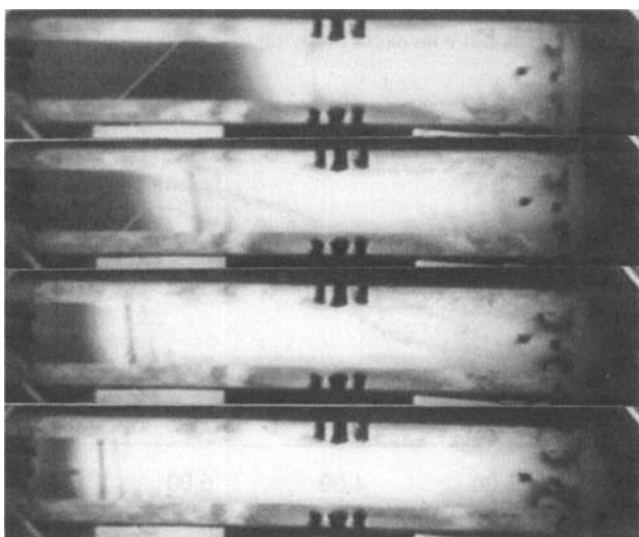


**FIGURE 4** The pictures showing the lines traveling toward the far end when exciter is moving to the right ( $V < 0$ ). They are taken from a MBBA cell at 25°C with  $V = -1.0$  mm/sec at four sequential stages. See Color Plate X.

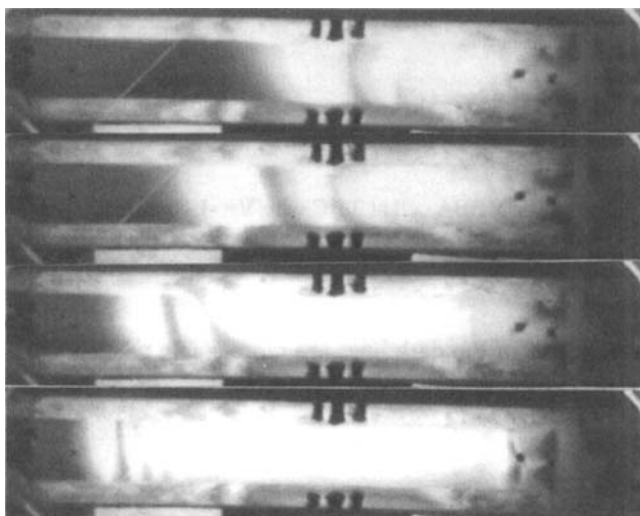


FIGURE 5 Same as Figure 4, but with exciter moving to the left ( $V = 1.0$  mm/sec). See Color Plate XI.

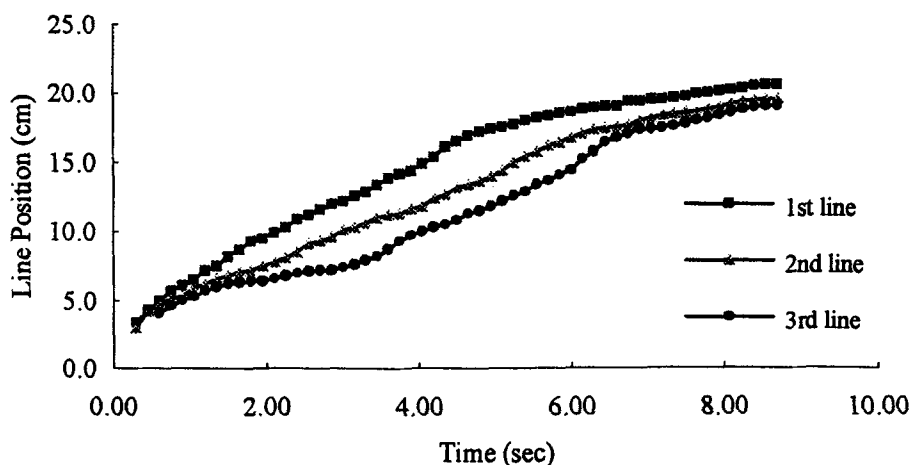


FIGURE 6 Time variation of the positions of the three dark lines in a MBBA cell at  $25^{\circ}\text{C}$  with  $V = 1.0$  mm/sec.

The dark lines move fast at beginning and slow down gradually. We show the time dependence of the dark line positions for the case with  $T = 25^{\circ}\text{C}$  and  $|V| = 1.0$  mm/sec in Figures 6 and 7. The velocity of the early appearing dark line approaches 78 mm/sec when time is 0.3 sec, which is much larger than  $V$ . In Figure 8, we show the first dark line velocity versus  $V$  for  $T = 30^{\circ}\text{C}$  when time  $t = 2.0$  sec.

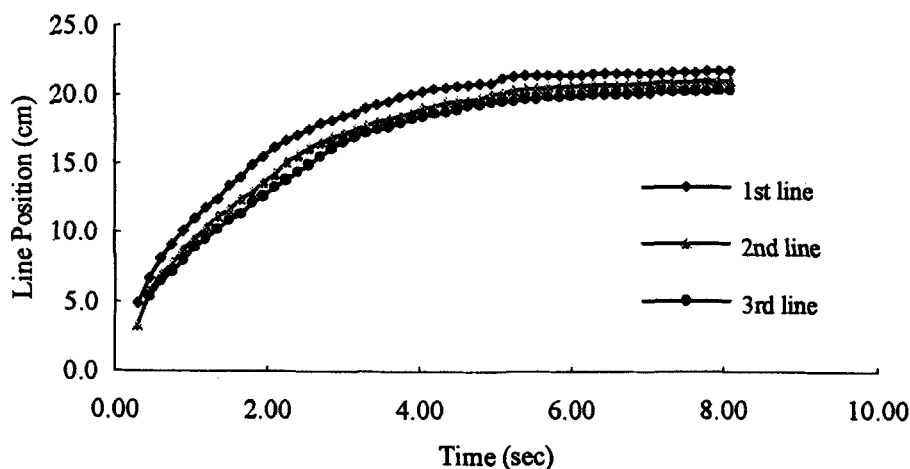


FIGURE 7 Time variation of the positions of the three dark lines in a MBBA cell at 25°C with  $V = -1.0$  mm/sec.

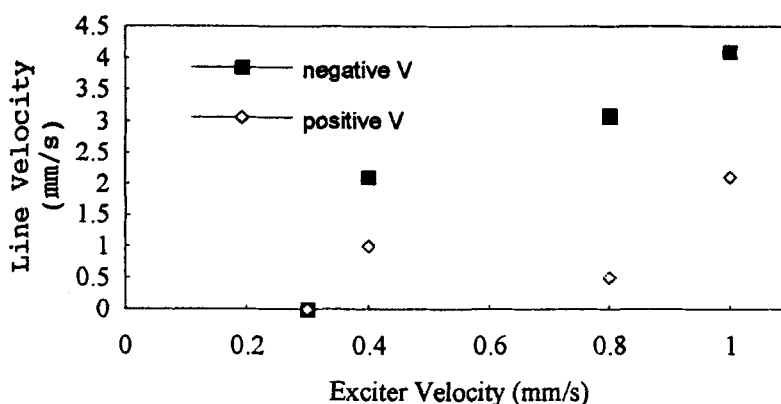


FIGURE 8 Variation of velocity of the first dark line versus the exciter velocity  $|V|$ . This is from a MBBA cell at 30°C, and the velocity is taken at  $t = 2.0$  sec after the exciter starts moving.

When we start moving the exciter either forward or backward, we always observe the dark lines moving toward the positive x-direction. When the moving exciter is stopped, we also observe dark lines with different widths appearing near the exciter (see Figure 9). However, these lines do not propagate toward the far end, rather they move backward and disappear one after another. They are darker and wider than those lines generated when the exciter is started moving from rest.



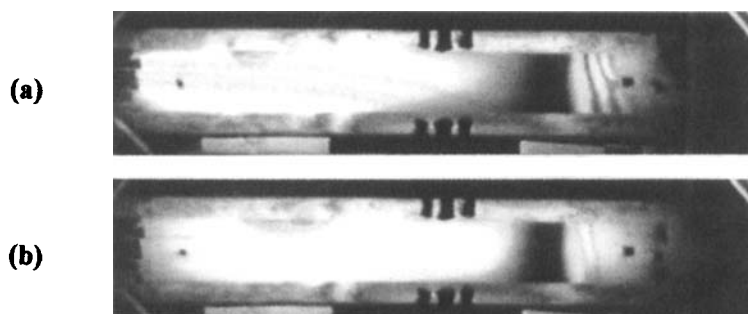


FIGURE 9 The dark lines are induced when the exciter motion is turned off. The lines can be observed clearly near the exciter end. The exciter is moving with (a)  $V < 0$  and (b)  $V > 0$ , respectively, before it is turned off. This is from a MBBA cell at  $26^\circ\text{C}$ . See Color Plate XII.

### Waves in 5CB cell

The 5CB cell is made with  $35.5\ \mu\text{m}$  spacer mylar films,  $23\ \mu\text{m}$  side mylar films, and  $18.8\ \mu\text{m}$  exciter mylar film. The temperature of the cell is fixed between  $22^\circ\text{C}$  and  $32^\circ\text{C}$ .

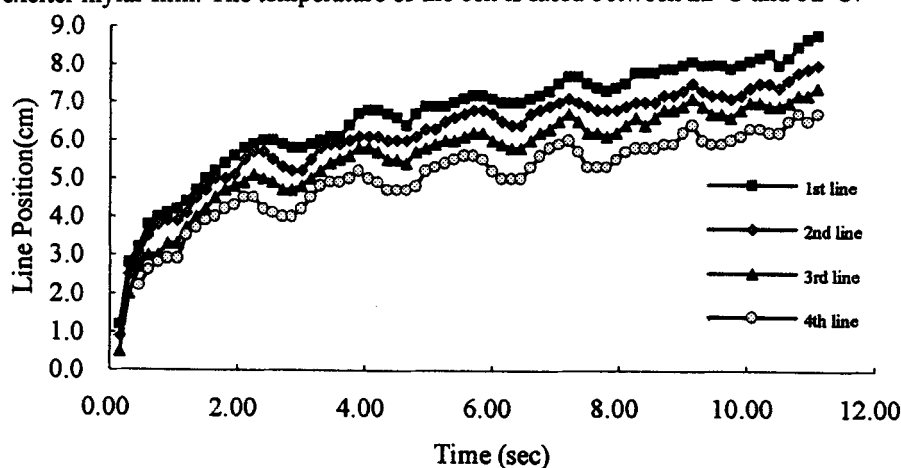


FIGURE 10 Time variation of the positions of the dark lines in 5CB cell at  $25^\circ\text{C}$  with  $V = 0.5\ \text{mm/sec}$ .

The exciter velocity  $|V|$  is fixed between  $0.2\ \text{mm/sec}$  and  $2.5\ \text{mm/sec}$ . The dark lines can be observed clearly. However, these lines in the 5CB cell are different from the traveling dark lines in the MBBA cell. They move back and forth, alternately. As an example, the line positions versus time curves are shown in Figure 10. The net displacements of dark lines are still forward. Even when  $|V|$  approaches  $2.5\ \text{mm/sec}$ , which is more than twice the highest velocity for the MBBA cell, the dark lines still cannot travel to the far end of the cell as those in the MBBA cell.

We find that the shapes of the dark lines are more stable when  $V > 0$  than when  $V < 0$ . This phenomenon is opposite to that in the MBBA cell. When  $|V|$  is reduced to smaller values, the dark lines disappear during the experimental process.

When the exciter begins to move, the dark lines move toward the far end for both  $V > 0$  and  $V < 0$ . When the exciter is stopped, the dark lines also appear near the exciter end and then disappear. These observations are similar to those found in the MBBA cell.

In one experiment in the 5CB cell, the cell temperature is increased until the middle of the cell, which always has a slightly higher temperature than the two end-regions, is in the isotropic liquid phase while the two end-regions are still in the nematic phase. The exciter is moved as before (either  $V > 0$  or  $V < 0$ ) and the dark lines are generated near the exciter and move to the middle of the cell. Since this middle part is in the isotropic liquid phase, it is all dark and the lines disappear in this region. After a while the lines appear in the other end as if they have penetrated through the middle isotropic liquid phase region and continue to move. The lines before and after the penetration are shown in Figure 11.

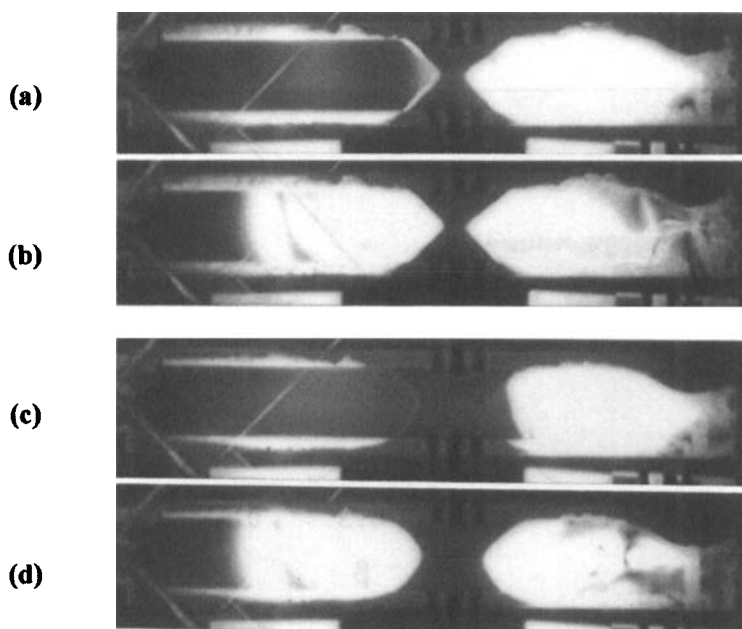


FIGURE 11 Penetration of the dark lines through an isotropic liquid region, the dark region in the center. In (a) and (b), the lines before and after the penetration, respectively, are shown. (c) and (d) show a similar phenomenon but the cell is at a slightly higher temperature. See Color Plate XIII.

## V. DISCUSSIONS

Some of our results from MBBA cell are similar to those observed in Ref. 8. For example, (i) three dark lines appear; (ii) the dark lines move toward the positive  $x$ -direction for both  $V>0$  and  $V<0$ ; (iii) the width of the early dark line is larger than that of the later one; and (iv) the dark line width decreases with time. We note that (ii) has been explained satisfactorily by the theory of Lam et al.<sup>3</sup>, and (iii) and (iv) are understood by considering the three dark lines as a multisoliton.<sup>10</sup> However, (i) remains unexplained; i.e., why there are three but not two or one dark line?

The fact that a whole dark region exists at the left end of the cell, which recedes as the dark lines move toward it (see Figures 4 and 5), indicates that the Poiseuille flow is not set up uniformly across the cell length. In other words, we are dealing with a nonuniform Poiseuille flow here, which may not even be steady. Consequently, the theory for a steady uniform Poiseuille flow outlined in Sec. III is not strictly applicable to our situation, but could still be approximately valid assuming that the flow in the bright region on the right where the dark lines travel is almost uniform and steady.

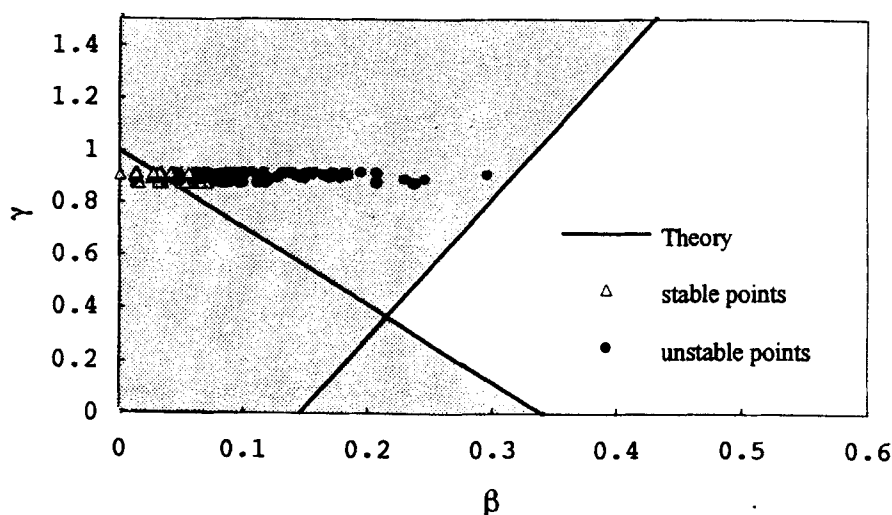


FIGURE 12 The "phase" diagram for nonlinear waves in 5CB cell. The two lines are from Ref. 11; the shaded area is where solitons are expected.  $\Delta$  corresponds to the conditions where we see stable waves, and  $\bullet$  is where we see unstable waves.

In contrast to the results in Ref. 8, except for the first and second dark lines in a limited time period (2-5 sec and 2-6 sec, respectively) as shown in Figure 6, the velocities of our dark lines are never constants. This implies that the dark lines are not

truly traveling waves; they are some nonlinear localized waves. The waves are nonlinear because the dark-line width decreases with time (see the remark on p.109 of Ref. 9).

With these qualifications in mind, we plot in Figure 12 the  $(\beta, \gamma)$  points from 5CB cell for both the stable dark lines which do not disappear during the experiments and the unstable dark lines which do disappear during the experiments. The values of  $K$  (by averaging  $K_{11}$  and  $K_{33}$ ),  $\gamma_1$  and  $\gamma_2$  are taken from Skarp et al.<sup>13</sup> The values of  $\beta$  and  $\gamma$  are calculated for each experiment with these constants and the assumption of  $U=V$ . Since the  $\gamma$  value of the 5CB nematic is in the range from 0.8 to 0.9, our experiments are limited in the  $\gamma$  range. Although we cannot observe the reentrant phenomenon as predicted by Lam, our results are consistent with his phase diagram in that all experimental points for the nonlinear waves do lie within the soliton region. To study the reentrant soliton phenomenon, we need to search for proper nematics with  $\beta$  and  $\gamma$  in a larger range and to generate a truly traveling wave.

Some other features of the dark lines could be understood qualitatively. Since the 5CB cell is thinner than the MBBA cell, the strong anchoring at the cell plates will make the molecules in the 5CB cell more difficult to flow and reorient than those in the MBBA cell. This explains why, in the 5CB cell, it takes a much larger exciter action to generate the dark lines and why the dark lines cannot travel as far as those in the MBBA cell for the same  $V$ . To have a quantitative comparison between the two cells, a similarity analysis<sup>9</sup> with every quantity, including  $V$ , expressed in dimensionless form is needed. This remains to be done.

The fact that the dark lines are more stable for  $V<0$  ( $V>0$ ) in the MBBA cell (5CB cell) probably is related to the flow conditions near the exciter, which could be very complicated to analyze due to the open edges of the cell at that location. To avoid this complication, a more closed cell (with a different soliton-generating mechanism) such as the split-plate cell proposed by Lam et al. in Ref. 10, could be a better choice.

It is interesting to note that in the two top pictures of Figure 5, the first and the second dark lines do start as symmetrical convex curves before they deform into inclined straight lines at later time. We observe that in all our experiments the dark lines always inclined in the same direction, with the top end traveling faster than the lower end. At this point, it is not clear whether this inclination of the dark line is due to any sideways asymmetry existing in the cell and/or the mechanical part of pushing the exciter, or any intrinsic hydrodynamic instability of the nematics. Note that the effect of the side boundaries of the cell has never been considered theoretically.<sup>9</sup> We do not know whether the dark lines are inclined or not in Zhu's experiment, because only the central parts of the dark lines were shown.<sup>8</sup> On the other hand, in the pressure-gradient generated dark lines observed by Lam and Shu,<sup>9</sup> the whole cell is shown and the dark

lines there are indeed inclined (see Figure 3.30 in Ref. 9). More experimental and theoretical studies are needed to clarify this issue.

Assuming that the Poiseuille flow in the bright region where the dark lines travel could be approximated as two layers of shear flow, as is done in Ref. 3, and the flow there is steady, we then have the case of steady nonuniform shear in this region. The theoretical results in Sec. 3.5.3 of Ref. 9 can thus be compared with our experiments. Since the maximum flow velocity—and hence the shear—in the bright region must be a decaying function of  $x$ , the case considered in Figure 3.40 of Ref. 9, one would expect that the velocity of the dark line to decrease with time. This is indeed the case for the first and second dark lines in Figure 6 and the three lines in Figure 7, but the behaviors of the third dark line in Figure 6 and those in Figure 10 are different. In particular, the oscillating of the dark line velocities between positive and negative values as shown in Figure 10 for the 5CB cell remains a puzzle. Oscillating velocity of the dark line under a time-dependent shear is found before<sup>14</sup> when the exciter is oscillating, but the velocity never goes to negative value in that case.

## VI. CONCLUSIONS

In our experiments we find that both temperature and the exciter velocity will affect the distances that the traveling dark lines can reach. In general the higher the temperature and the exciter velocity, the farther away from the origin the dark lines can travel, but the exciter velocity has much more influence on the dark lines than the temperature. The nonlinear waves propagate toward the positive  $x$ -direction when the exciter moving either forward or backward, but the time-position relations are different in these two cases (see Figures 6 and 7). The wave behavior is also affected by the direction of the exciter velocity. This result is different from Zhu's experiment.<sup>8</sup> Finally, the director wave penetrating through the isotropic liquid phase region suggests that it may be possible to generate solitary waves in the isotropic liquid phase, a topic worth more theoretical and experimental studies.

## ACKNOWLEDGMENTS

This work is supported by the National Science Council of the Republic of China under grant NCS82-0208-M009-026.

## REFERENCES

1. P. G. de Gennes and J. Prost, The Physics of Liquid Crystals (Clarendon Press, Oxford, 1993).
2. S. Chandrasekhar, Liquid Crystals (Cambridge University, Cambridge,

- 1992) .
3. L. Lin (L. Lam), C. Q. Shu, J. L. Shen, Y. Huang, and P. M. Lam, Phys. Rev. Lett., **49**, 1335 (1982); **52**, 2190 (1984) .
4. L. Lin and C. Q. Shu, Chin. Phys., **4**, 598 (1984) .
5. L. Lin, C. Q. Shu, and G. Xu, Phys. Lett., **109A**, 277 (1985) .
6. C. Q. Shu and L. Lin, Mol. Cryst. Liq. Cryst., **131**, 47 (1985) .
7. L. Leger, Solid State Commun., **11**, 1499 (1972) ;  
Mol. Cryst. Liq. Cryst., **24**, 33 (1973) .
8. Zhu Guozhen, Phys. Rev. Lett., **49**, 1332 (1982) .
9. L. Lam and C. Q. Shu, in Solitons in Liquid Crystals, edited by L. Lam and J. Prost (Springer, New York, 1992) .
10. L. Lin, C. Q. Shu, and G. Xu, J. Stat. Phys., **39**, 633 (1985) .
11. L. Lam, Liquid Crystals, **14**, 1873 (1993) .
12. F. J. Kahn, Appl. Phys. Lett., **22**, 386 (1973) .
13. K. Sarp, S. T. Lagerwall, and B. Stebler, Mol. Cryst. Liq. Cryst., **60**, 215 (1980) .
14. G. Xu, C. Q. Shu, and L. Lin, Phys. Rev., **A36**, 277 (1987) .